Astrocytic mitochondrial transfer to brain endothelial cells and pericytes *in vivo* increases with aging

Gopal V Velmurugan[1,2] ⓘ, Hemendra J Vekaria[1,2,3],
Samir P Patel[1,3], Patrick G Sullivan[1,2,3] and
W Brad Hubbard[1,3,4] ⓘ

Abstract

Intercellular mitochondrial transfer (IMT) is an intriguing biological phenomenon where mitochondria are transferred between different cells and notably, cell types. IMT is physiological, occurring in normal conditions, but also is utilized to deliver healthy mitochondria to cells in distress. Transferred mitochondria can be integrated to improve cellular metabolism, and mitochondrial function. Research on the mitochondrial transfer axis between astrocytes and brain capillaries *in vivo* is limited by the cellular heterogeneity of the neurovascular unit. To this end, we developed an inducible mouse model that expresses mitochondrial Dendra2 only in astrocytes and then isolated brain capillaries to remove all intact astrocytes. This method allows the visualization of *in vivo* astrocyte- endothelial cell (EC) and astrocyte-pericyte IMT. We demonstrate evidence of astrocyte-EC and astrocyte-pericyte mitochondrial transfer within brain capillaries. We also show that healthy aging enhances mitochondrial transfer from astrocytes to brain capillaries, revealing a potential link between brain aging and cellular mitochondrial dynamics. Finally, we observe that astrocyte-derived extracellular vesicles transfer mitochondria to brain microvascular endothelial cells, showing the potential route of *in vivo* IMT. These results represent a breakthrough in our understanding of IMT in the brain and a new target in brain aging and neurovascular metabolism.

Introduction

Intercellular mitochondrial transfer (IMT) is a pivotal aspect of intercellular communication in multicellular organisms, initially recognized two decades ago.[1] IMT is a unique process by which mitochondria or mitochondrial DNA transfer between cells.[2] Unlike mitochondrial transmission during cell division, IMT does not follow the traditional inheritance pattern and can occur between cells of the same organism or between different species.[1,2] IMT has been observed in multiple contexts, such as cellular stress responses, injury, and cancer progression, where it aids in restoring mitochondrial function, enhancing cellular bioenergetics, and modulating cellular repair mechanisms.[1–4]

Research has been conducted to reveal the methods of mitochondrial transfer between cells. *In vitro* studies reveal tunneling nanotubes (TNTs) facilitate transfer of various organelles, including Golgi, endoplasmic reticulum, and mitochondria, among others, from donor cells like fibroblasts, astrocytes, macrophages and

[1]Spinal Cord and Brain Injury Research Center, University of Kentucky, Lexington, KY, USA
[2]Department of Neuroscience, University of Kentucky, Lexington, KY, USA
[3]Lexington Veterans' Affairs Healthcare System, Lexington, KY, USA
[4]Department of Physiology, University of Kentucky, Lexington, KY, USA

Corresponding authors:
W Brad Hubbard, 467 Biomedical & Biological Sciences Research Bldg, 741 South Limestone St Lexington, KY, USA.
Email: bradhubbard@uky.edu

Gopal V Velmurugan, 478A Biomedical & Biological Sciences Research Bldg, 741 South Limestone St Lexington, KY, USA.
Email: vetvelu@uky.edu

cardiomyocytes, to acceptor cells such as endothelial cells (ECs), neurons, and cancer cells.[1,5–11] Additionally, donor cells can produce extracellular vesicles loaded with mitochondria (EV-Mito), which then are transferred to acceptor cells.[12] Notably, free mitochondria and EV-Mito[13,14] in circulation migrate over considerable distances, entering cells in different tissues, e.g., from adipose tissue to the heart [15] or heart mitochondria to brain endothelial cells.[16] In lungs, mesenchymal and bone marrow-derived stem cells transfer mitochondria to airway epithelial cells, mitigating injury and inflammation.[17,18]

A seminal study demonstrated that astrocytes have the ability to deliver mitochondria to neurons in the context of ischemic stroke, in efforts to improve neuronal recovery.[19] However, IMT can be hijacked to promote tumorigenic potential of cancer cells.[20,21] It is also evident that mitochondrial transfer not only occurs in cancer and other pathologies but also under physiological conditions. Metabolically-active cells like cardiomyocytes transfer dysfunctional mitochondria in vesicles to resident macrophages for final disposal to maintain mitochondrial fitness of cardiomyocytes.[11] Similarly, neuron-astrocyte mitochondria transfer axis can represent a transmitophagy process, where astrocytes dispose of neuronal mitochondria.[22] In the cardiovascular system, mitochondrial exchange between embryonic cardiomyocytes and mesenchymal stem cells aids differentiation and proliferation, offering therapeutic potential in cardiovascular disorders.[23] Also, studies have shown that mitochondrial transfer from vascular smooth muscle cells to mesenchymal stem cells is required to promote stem cells proliferation.[23]

Numerous studies have explored IMT across various organ systems, yet investigations in the central nervous system (CNS) remain limited, largely due to the complex heterogeneity of its cellular composition. Crucially, in vivo methods that assess mitochondrial transfer are more physiologically relevant for studying mitochondrial exchange between brain cells. The neurovascular unit (NVU), the fundamental functional unit of the CNS, is composed of vascular cells (endothelial cells and pericytes), glial cells (astrocytes), and neurons. An integral component of the NVU is the blood-brain barrier (BBB), comprised of tight junctions between endothelial cells, pericytes, and astrocyte end-feet closely intertwined to maintain barrier integrity.[24–26] The close association between end-feet astrocytic mitochondria and endothelial cells senses hypoxia and the regulate vascular tone and cerebral blood flow.[27,28] Recent evidence suggests that mitochondrial transfer is central to intercellular communication between cells in the BBB.[29,30]

To this end, there may be an underappreciated role of astrocytes to dictate neurovascular metabolism and

IMT may be an avenue for this type of cellular communication. In this study, we utilize a tamoxifen (TAM)-inducible mouse model which expresses green-fluorescence Dendra2 (mtD2) specifically in astrocyte mitochondria to examine mitochondrial transfer from astrocyte to brain microvascular endothelial cells (BMEC) and pericytes in purified brain capillaries. We also investigate the astrocyte-brain capillary IMT in the context of healthy aging and extracellular vesicle-mediated delivery of astrocyte mitochondria as a method of IMT transfer.

Methods

Animal

All studies were approved by the University of Kentucky Institutional Animal Care and Use Committee (IACUC), accredited by the Association for the Assessment and Accreditation of Laboratory Animal Care International (AAALAC International). All experiments were conducted in compliance with the ARRIVE guidelines and in strict accordance with the National Institutes of Health (NIH) Guide for the Care and Use of Laboratory Animals (NIH Publication No. 8023, revised 2011). All the mice were bred and maintained at Division of Laboratory Animal Resources (DLAR) at the University of Kentucky. Mice (B6;129S-Gt (ROSA)26Sortm1.1 (CAG-COX8A/Dendra2) Dcc/J) expressing a mitochondrial-specific version of Dendra2 green (mtD2; heterozygous) was used as globally-expressing mtD2 (Strain#: 018397). A tamoxifen inducible mouse model which expresses green-fluorescence dendra2 (mtD2) specifically in astrocyte mitochondria (Ast-mtD2) was generated by crossing Mice B6;129S-Gt(ROSA)26Sortm1(CAG-COX8A/Dendra2)Dcc/J (Jax #018385) with B6N.FVB-Tg (Aldh1l1-cre/ERT2)1Khakh/J (Jax #031008). Cre-positive animals were injected with tamoxifen (75 mg/kg BW) at 6–8 weeks age for five consecutive days. Mice were sacrificed at one (young mice) and five months (healthy aged mice) after tamoxifen injection, which was performed when mice where 2 months old, to assess mitochondrial transfer from astrocyte to brain capillaries.

Brain capillary isolation

Mouse brain capillaries were isolated as described previously.[31] After euthanasia with CO_2, mouse brains were collected in ice-cold capillary isolation buffer (DPBS; Cat No: 14080055, Fisher Scientific with 5.5 mM glucose, 1 mM sodium pyruvate, and 1% BSA with pH 7.4), homogenized into small pieces using a razor blade and transferred into a 2 mL

screw-cap tube (Sarstedt Inc Screw Cap Microtube, type H) preloaded with stainless beads (3.2 mm, 1.8 g, fisher scientific, NC0778455). Further homogenization was done with 1 ml of ice-cold capillary isolation buffer in bead homogenizer (Biospec products) for 15 seconds and transferred into a 5 ml conical tube and the volume was made to 5 ml using isolation buffer. Homogenate was vortexed for 30 seconds and centrifuged at $1000 \times g$ for 10 min at 4°C in a swinging bucket rotor. The supernatant was removed carefully, and 4 mL of lymphocyte separation medium (25-072-CV; Corning Life Sciences) was added to the pellet to separate the brain vessels from myelin and other brain cells by gradient centrifugation. The homogenate was vortexed for 30 seconds to obtain a homogenous suspension and samples were centrifuged at $4500 \times g$ for 20 min at 4°C using a swinging bucket rotor. The top myelin layer was removed along with the supernatant, and the inner sides of the tube were cleaned to remove leftover myelin debris using Kim Wipes or cotton buds. The pellet was resuspended in 1 ml of ice-cold isolation buffer, and the resulting homogenate was filtered through a 70 μm membrane filter (15-1070; Tisch Scientific), and washed with a minimum of 10 ml of isolation buffer to separate capillaries from larger vessels. The filtrate was then filtered through an 18 μm membrane (25 mm diameter) filter (ME17233; Tisch Scientific). and washed with a minimum of 10 ml of isolation buffer to separate to wash the capillaries from cells and debris. Finally, the membrane filter with capillaries on the top was removed quickly from the filter holder and placed inside the 1 ml microcentrifuge tube wall. Using a 1 ml pipette, all the capillaries were eluted from the membrane by flushing 1 ml of wash buffer 2–3X or by quick vortex. Around 100 μl of capillary suspension was used on a glass slide to adhere for one hour at room temperate (RT) and fixed with 10% neutral buffered formalin (NBF) before immunostaining procedure.

Immunofluorescence

Immunostaining was done as described previously with modification.[32] NBF fixed brain capillary samples, cells and brain sections were permeabilized, and blocked together in 0.2% Trion X-100 in TBST + 1%BSA and 10% normal horse serum for one hour at RT. To stain plasma membrane, cells were treated with wheat germ agglutinin (5 μg/ml) conjugate (Thermofisher; W11262) before permeabilization. Then, the sections were incubated overnight at 4°C with primary antibody (1:250 dilution; Table 1) in antibody dilution buffer (blocking buffer and PBST at 1:1 ratio). Followed by fluorophore-labelled secondary antibody (1:500 dilution; Table 1) at RT for 1 h. After washing, the samples were mounted on glass slides using Vectashield antifade mounting medium with or without DAPI (H-1500 and H-1400; Vector laboratories, USA).

Confocal imaging and image processing

Fluorescence Z-stack images were acquired using a confocal microscope (Nikon A1R or Nikon AXR; 20X air, 60X oil and 100X oil) or widefield fluorescent microscope (Nikon Ti2; 20X air and 60X water) and processed using NIS-Elements version 5.30.05. Z-stack images were denoised and sometimes deconvoluted to increase resolution. 3D images were reconstructed using Z-stack images in NIS-elements or using Imaris (10.0.0) as explained previously.[32] General analysis 3 (GA3) in NIS-elements was used to analyze total volume of capillary and Dendra2 using confocal z-stack images (capillary- Isolectin; Dendra2- green). From this percentage volume of denera-2 coverage on

Table 1. Primary and secondary antibodies.

S.No	Primary antibody	Vendor	Catalogue number	Dilution
1	TOM-20	Cell Signaling	42406S	1:250
2	GFAP	Cell Signaling	80788	1:250
3	RBFOX3/NeuN	Novus biologicals	NBP1-92693	1:250
4	MAP-2	Thermofisher	MA1-25044	1:250
5	AQP4	Cell Signaling	59678S	1:250
6	Griffonia Simplicifolia Lectin I (GSL I) isolectin B4, Biotinylated	Vector Laboratories	B-1205-.5	1:250
	Secondary antibody			
1	Alexa flour 350 goat anti-Rabbit	Thermofisher	A11046	1:500
2	Alexa Flour 488 goat anti-mouse	Thermofisher	A11001	1:500
3	Alexa flour 594 donkey anti-mouse	Thermofisher	A-21203	1:500
4	Alexa flour 594 donkey anti-rabbit	Thermofisher	A21207	1:500
5	Alexa flour 488 donkey anti-rabbit	Thermofisher	A-21206	1:500
6	DyLight*649 STREPTAVIDIN	Vector Laboratories	SA-5649-1	1:500

isolated capillaries (normalized to total capillary volume) were calculated.

Astrocyte cell culture and astrocytic EV-Mito enrichment

Primary astrocytes were cultured from P0-1-day-old wild-type or Ast-mtD2 pups as previously described, with slight modifications.[33,34] Briefly, after removing the meninges, the brain cortex was dissected into smaller pieces and digested with 0.05% trypsin for 15–20 minutes at 37°C, with gentle shaking every 5 minutes. The trypsinization was neutralized using DMEM supplemented with 10% FBS, followed by gentle trituration (∼15–20 times) to dissociate the tissue. The suspension was allowed to settle for 1 minute to separate debris, and the supernatant was filtered through a 70 μm cell strainer before centrifugation at 300 g for 5 minutes at room temperature. The resulting cell pellet was resuspended and plated in T-75 flasks containing high-glucose DMEM supplemented with 10% FBS and antibiotics (ThermoFisher; 15-140-122). After 12 hours, the medium was replaced with astrocyte culture medium (ScienceCell; MSPP-1801), which was subsequently changed every 3 days. Upon reaching confluency (8–10 days), primary astrocytes were isolated by removing glial cells through orbital shaking at 200 rpm for 6 hours. Finally, the astrocytes were dissociated using trypsinization and sub-cultured for further experiments. After four days, primary astrocyte conditioned media was centrifuged at 13,000 g for 30 minutes at 4°C to enrich astrocytic EV-Mito. The pellet was resuspended in 400 μl media from each T75 flask and 100 μl of enriched EV-Mito aliquot was used in four well chamber slides for mitochondrial transfer experiments.

Endothelial cell culture

All cells were cultured at 37°C with 5% CO_2 in the incubator. Rat primary BMECs (Cell applications Inc; R840-05a) and mouse BMECs (Cell biologicals; C57-6023) were cultured using endothelial cell growth medium (PromoCell; CC22011) with required supplements. BMECs were cultured in glass bottom chamber slide (Cellvis; C4-1.5P), 24 hours before the addition of mtD2 astrocyte EV-Mito for mitochondrial transfer experiments.

Live cell imaging

Primary BMECs were cultured in glass bottom chamber slide before the addition of mtD2 astrocyte EV-Mitos. EV-Mitos were mixed gently using a pipette. After 48–72 hours of incubation, cells were washed three times with warm media. BMECs were stained with MitoTracker deep red-FM (500 nM) as per manufacturers direction (ThermoFisher; M22426) for 15 minutes at 37°C. Hoechst dye (1ug/ml) was added to BMECs for 3 minutes. Finally, cells were washed twice with warm media before imaging in 60X oil for 5–10 minutes for every 5 seconds to monitor transfer astrocyte mtD2 mitochondria (green) and endogenous mitochondria (pink). In a subset of experiments, live cells were imaged only with Hoechst dye without staining endogenous mitochondria with MitoTracker red.

Statistics

Statistical analysis was performed using Graph Pad Prism (GraphPad Software, CA, USA). A significant difference among groups was defined as $p < 0.05$ for all analyses. The Shapiro-Wilk test was completed to ensure normality. As these criteria were met for all experimental data, parametric statistics were employed for all analyses. A two-tailed, unpaired t-test was used to examine mitochondrial transfer.

Results

Generation and characterization of astrocyte-specific mitochondrial reporter mice (ast-mtD2)

To examine mitochondrial transfer from astrocytes to brain capillaries, we generated Ast-mtD2 mice (Figure 1(a)). Brain sections and isolated brain capillaries were analyzed to assess tissue-specific expression of mtD2. In the absence of tamoxifen administration, no mtD2 expression was observed in brain sections (data not shown). However, tamoxifen administration specifically induced mtD2 expression in astrocyte mitochondria (Figure 1(b)), with no expression in neurons. Due to the tight association of cells in the neurovascular unit (astrocytes, neurons, and capillaries), visualizing *in vivo* mitochondrial transfer from astrocytes to brain capillaries is challenging. Therefore, we isolated brain capillaries as described in the methods section to facilitate the visualization of mitochondrial transfer.

Isolated brain capillaries have minimal astrocyte remnants that do not retain astrocyte mitochondria

We first tested whether the isolated brain capillary pool from young mice contained astrocyte remnants by staining with glial fibrillary acidic protein (GFAP) and aquaporin-4 (AQP-4). Our isolation method shows that the isolated capillaries contain few instances of the astrocyte marker GFAP (∼5% of isolated brain capillaries contain GFAP+ remnants) (Figure 2(a) to (d)). However, a majority of brain capillaries
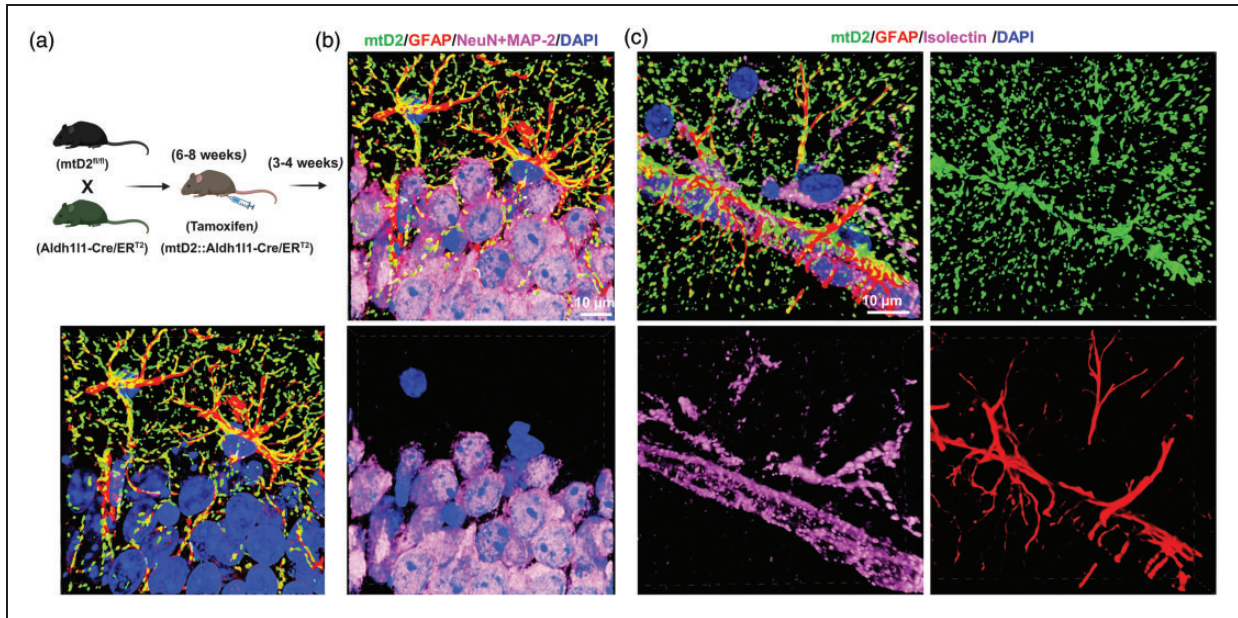
Figure 1. Generation and characterization of astrocyte-specific mitochondrial reporter mice (Ast-mtD2). (a) Breeding scheme for the generation of astrocyte specific mitochondrial reporter (Dendra2; green) mice (Ast-mtD2) that express fluorescently-labeled mitochondria (mtD2) after tamoxifen injection. (b) Representative immunostained confocal images (cropped, denoised 3D image) from Ast-mtD2 brain section after 4 weeks of tamoxifen injection (neuron-pink; astrocyte-red; nucleus-blue and endogenously expressing mtD2-green) and (c) representative brain section immunostained for astrocyte-red; capillaries-pink; nucleus-blue and endogenously expressing mtD2-green (cropped, denoised 3D image).
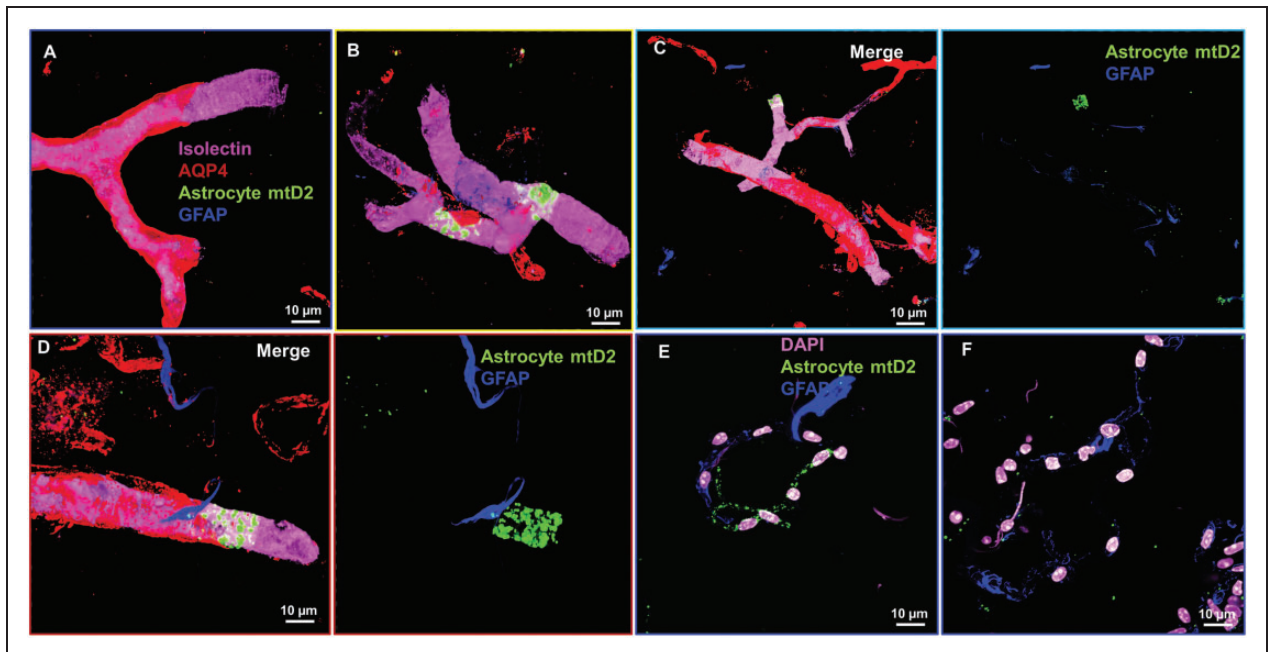

Figure 2. Astrocytic end-feet and membranes do not retain astrocyte mitochondria in isolated brain capillaries: Immunostained confocal images from Ast-mtD2 mouse brain capillaries from young mice show very few astrocyte remnants (blue) in the isolated brain capillaries and most of them not co-localized with astrocyte mitochondria (green). (a–d) Representative confocal, denoised 3D reconstructed images of isolated brain capillaries stained for brain vascular endothelial cells (Isolectin; pink), astrocyte (GFAP; blue) and astrocyte end-feet (AQP4; red). Astrocyte expresses mtD2 endogenously after tamoxifen injection. (e, f) Representative micrographs of brain capillaries stained for astrocyte (blue) and nucleus (pink) and mtD2 (green) expressed endogenously.

were positive for AQP-4 (Figure 2(a) to (d)). Importantly, capillaries positive for either GFAP or AQP-4 did not show astrocyte mtD2 expression that colocalized with GFAP or AQP-4[31] (Figure 2(a) to (f)), confirming that the remaining portions of astrocytic processes and end-feet do not contain any astrocyte mitochondria. Astrocytic mtD2 was found below the AQP-4 layer and within the capillary endothelial cell layer where no AQP-4 was present (Figure 2(c) and (d)).

Astrocytic mitochondrial transfer to brain microvascular endothelial cells

We further investigated astrocyte mitochondrial transfer into BMECs in young mice using NIS-Elements and Imaris image processing software. Planar XY and YZ confocal image projections of isolectin (pink) and astrocyte mtD2 (green) showed merged signals (Figure 3(a)). A three-dimensional (3D) view of the same capillary, obtained by confocal microscopy, revealed astrocyte mtD2 localized within the EC layer (pink), situated below the AQP4 layer (red) and surrounding the EC nucleus (blue) (Figure 3(b) and (c)). From the average total capillary volume, around 3% of the capillary volume had transferred astrocyte mitochondria (Figure 3(d)). Imaris-processed 3D image of the same capillary confirmed the presence of astrocyte mtD2 along the capillary layer of ECs (Figure 3(e)). To illustrate the appearance of endogenously expressed mtD2 in brain capillaries versus that observed from transferred mitochondria, we isolated capillaries from mice with global mtD2 expression and compared with Ast-mtD2 mice capillaries (Figure 3(f) and (g)). Confocal images showed similar localization of mtD2 in both Ast-mtD2 and global-mtD2 capillaries, though as expected, transferred mitochondria in Ast-mtD2 capillaries are a small subset of the total mitochondrial population. To further confirm, we stained Ast-mtD2 capillaries with TOM-20 and found that the locations where mitochondrial transfer occurred contained both endogenous mitochondria (red) and astrocyte-transferred mitochondria (yellow) (Figure 3(h) and (i)).
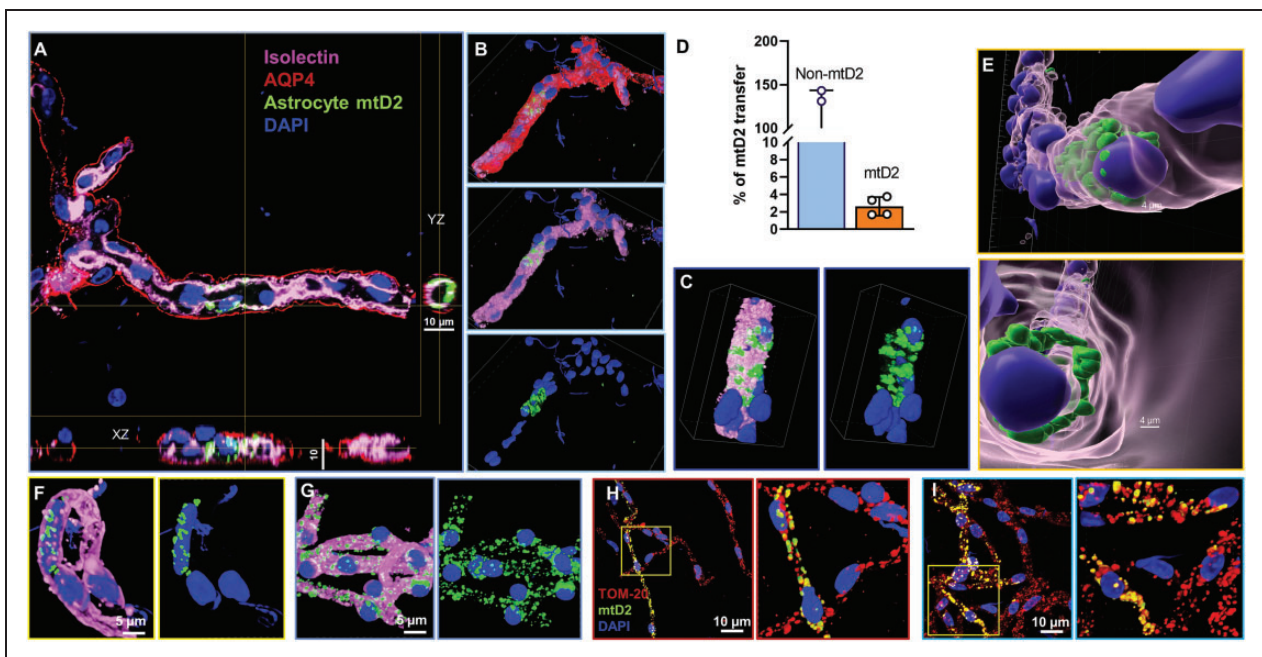

Figure 3. Detection of astrocytic mitochondrial transfer in brain microvascular endothelial cells. (a–e) Isolated brain capillaries from young Ast-mtD2 mice (astrocytic mitochondria; green) stained for brain endothelial cells (isolectin; pink), astrocyte end-feet (AQP4; red), and nucleus (DAPI; blue). (a) Representative confocal XY and YZ planes of brain capillary endothelial cells shows mitochondrial transfer from astrocytes. (b, c) Denoised, confocal 3D reconstruction images showing astrocyte mitochondrial transfer in brain capillary endothelial cells localized below astrocytic end-feet and around the endothelial nucleus. (d) Bar chart represents percentage of mitochondrial transfer from astrocyte to brain capillaries. Capillary and mtD2 volume was analyzed using in NIS-elements. Percentage of mitochondrial transfer calculated from average of four random microscopical field at 10X magnification. Data represented as mean ± SD. (e) 3D reconstruction z-stack images using Imaris to show astrocyte mitochondria (mtD2; green) is inside the capillary and around the endothelial nucleus. (f, g) Isolated brain capillaries from Ast-mtD2 (F) and Global-mtD2 (G) stained for brain endothelial cells (isolectin; pink) and nucleus (DAPI; blue). (h, i) Isolated brain capillaries from Ast-mtD2 mice (astrocytic mitochondria; green) stained for total mitochondria (TOM-20; red) and nucleus (DAPI; blue). Representative micrographs showing endogenous capillary endothelial cell mitochondria co-localized astrocyte mitochondria (colocalization; yellow) around the nucleus.

Astrocytic mitochondrial transfer to the pericyte soma

We also investigated astrocyte mitochondrial transfer to pericytes in young mice. Pericytes are specialized cells around the endothelium that appear as "bumps on a log" and can be recognized by this unique cellular anatomy relative to ECs. Isolectin staining clearly differentiates capillary endothelial wall from pericyte bump (Figure 4(a)) with astrocyte mitochondrial transfer. Planar XY and YZ confocal image projections of endogenous mitochondria (TOM20; red) and astrocyte mtD2 (green) showed merged signals (Figure 4(b)) and individual channels further shows the co-localization (yellow) of astrocyte mitochondria (green) and endogenous mitochondria (red) (Figure 4(c)). A 3D view of the same brain capillary, processed using NIS-elements and Imaris, revealed astrocyte mtD2 localized within the pericyte (capillary bump), along endogenous pericyte mitochondria. (Figure 4(d) and (e)). To compare the appearance of endogenously-expressed mtD2 in pericytes versus transferred mitochondria, we isolated capillaries from mice with global mtD2 expression and compared with Ast-mtD2 capillaries (Figure 4(f) and (g)). Confocal images show similar localization of mtD2 in both Ast-mtD2 and global-mtD2 capillaries, except that Ast-mtD2 in brain capillaries represent a subset of total mitochondria. To further confirm, we stained Ast-mtD2 capillaries with TOM-20 and found that astrocyte-transferred mitochondria (green) overlap with endogenous mitochondria (red) for distinct colocalization (Figure 4(f)).

Aging increases mitochondrial transfer from astrocytes to brain capillaries

Aging can result in neurovascular dysfunction and damage to BMECs.[35] Through healthy aging, we hypothesize that astrocyte can compensate for age-related BMEC mitochondrial deficits. Therefore, we tested whether healthy brain aging alters astrocytic IMT to brain capillaries. To test this, we injected TAM to induce mtD2 (green) expression in astrocytic mitochondria around 6–8 weeks of age before brain capillary isolation at either 3 months (1 month post-TAM) or 7 months (5 months post-TAM) (Figure 5(b)). Interestingly, we found increased percentage of mitochondrial transfer from astrocytes to capillaries in 7 months old mice compared to 3 months old mice (Figure 5(a) to (c)).
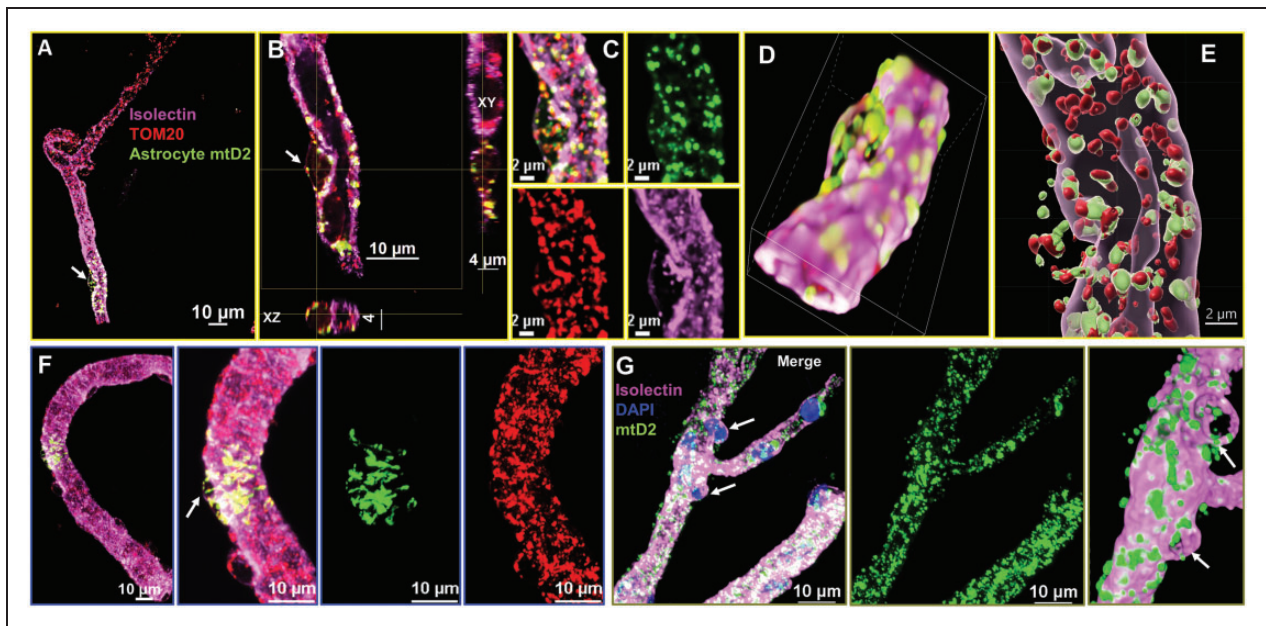

Figure 4. Detection of astrocyte mitochondrial transfer in pericytes: Immunostained confocal images ((denoised and cropped) from young Ast-mtD2 mouse brain capillaries showing astrocyte mitochondria (green) in pericytes and co-localized with pericyte mitochondria (red). (a–g) Isolated brain capillaries stained for brain vascular endothelial cells (isolectin; pink) and endogenous mitochondria (TOM-20; red); astrocyte mtD2 (green). (a–c) Representative confocal micrograph showing astrocyte mitochondria (green) co-localized with pericyte mitochondria (red) identified by the shape and location on the capillary. Confocal XY and YZ planes pericytes shows mitochondrial transfer from astrocytes. (d and e) Confocal 3D reconstruction images using NIS-elements and Imaris showing astrocyte mitochondrial transfer in pericyte. (f) Micrographs showing astrocyte mitochondrial transfer into pericytes in brain capillaries. brain vascular endothelial cells (isolectin; pink); endogenous mitochondria (TOM-20; red); astrocyte mtD2 (green) (g) capillaries isolated from Global-mtD2 mouse stained for capillary endothelial cells (isolectin; pink) and nucleus (blue).
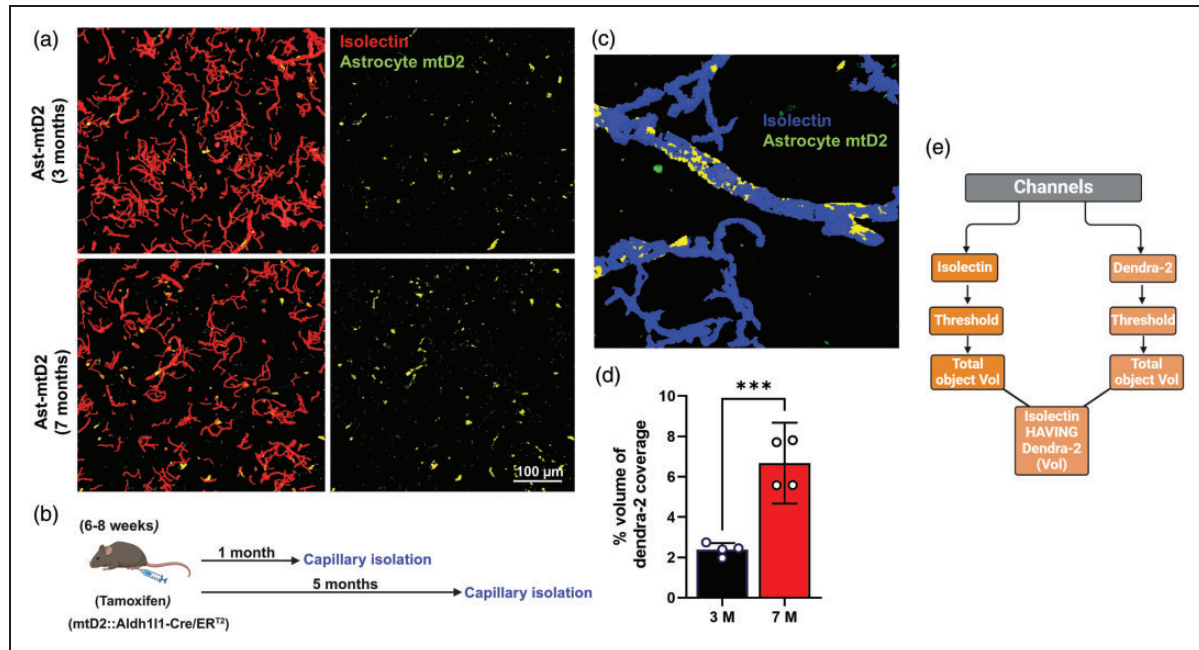
Figure 5. Aging increases mitochondrial transfer from astrocytes to brain capillaries: (a) Representative capillary micrographs from Ast-mtD2 mouse stained for vascular endothelial cell marker (Isolectin; red); astrocyte mtD2 (green). Top panel represents 3-month-old young mice-derived capillaries isolated one month after tamoxifen (TAM) injection to express mtD2 in astrocytes. Bottom panel represents 7-month-old healthy aged mice-derived capillaries isolated five months after TAM injection. (b) Schematic diagram represents the experimental paradigm for capillary isolation. (c) Representative micrograph generated using General analysis 3 (GA3) in NIS-elements to analyze the % volume of Dendra2 covered total volume of isolectin (capillary) volume. (d) Bar graph shows quantification of % volume of Dendra2 coverage on isolated capillaries (normalized to total capillary volume). Data represented as mean with effect size; R^2 value of 0.87 with 95% CI (2.6-5.8). $p \leq 0.01$ ***; using unpaired t-test and (e) flow chart represents how GA3 analysis was done to find % volume of Dendra2 using colocalization tool in NIS-elements.

Astrocyte-derived extracellular vesicles (EV-Mito) mediate mitochondrial transfer to brain microvascular endothelial cells

IMT can occur via several routes, including TNTs or EV-Mito.[1] To assess the potential of EV-Mito as the route of mitochondrial transfer between astrocytes and brain capillaries, we isolated EV-Mito from primary mtD2 astrocytes (Figure 6(a) and (b)) and wild-type astrocytes (Figure 6(c)) conditioned media. Presence of astrocyte mitochondria inside the vesicles is confirmed by the presence of mtD2 (Figure 6(b)). Staining of wild-type EV-Mito with dyes which stains for intact mitochondrial membrane potential (TMRE) and nucleus (DAPI) confirmed the vesicles contain astrocyte mitochondria, as opposed to nuclear fragments (Figure 6(c)). Live cell imaging of BMEC after 48 hours of incubation revealed the mitochondrial transfer of astrocyte mitochondria from EV-Mito into BMEC (Figure 6(d)). Further, co-culture of mtD2 astrocytes and BMECs demonstrates astrocytic mitochondrial transfer horizontally to BMEC (Figure 6(e)). Live cell imaging reveals that transferred mitochondria move within BMECs indicating the

functionality of transferred mitochondria (Video 1). We observe that transferred mitochondria do not fuse with the endogenous mitochondria pool for at least 72 hours after incubation.

Discussion

Astrocytic end-feet, which closely wrap around brain capillaries, form tight contacts with ECs and pericytes, which make it highly challenging to image and visualize mitochondrial transfer from astrocytes to capillaries in brain sections. To overcome this obstacle, we developed a strategy to isolate capillaries from Ast-mtD2 mice, allowing us to immunostain and image mitochondrial transfer in the presence of minimal astrocyte remnants. In this study, using a transgenic mouse model expressing mtD2 in astrocytes, we demonstrated that astrocytes transfer mitochondria to brain capillaries, including both ECs and pericytes under physiological conditions. We found that this mitochondrial transfer process increases with aging.

Our method to isolate brain capillaries allowed for more precise assessment of mitochondrial transfer into brain capillaries. Mitochondrial transfer was identified
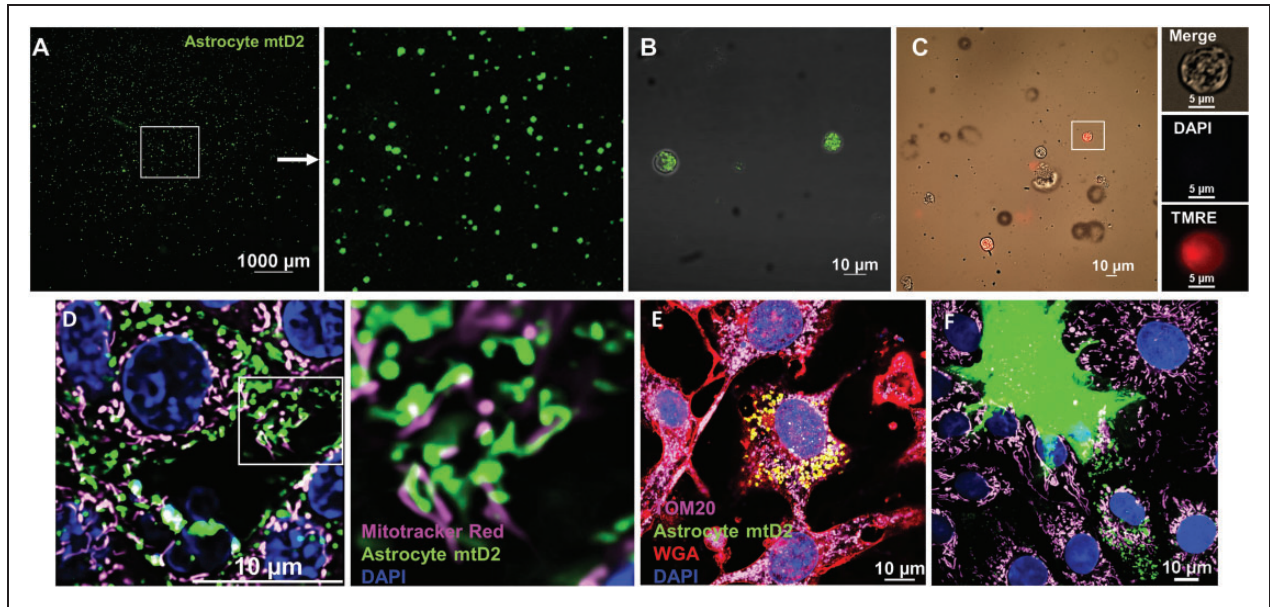
Figure 6. Astrocytic extracellular vesicles containing mitochondria (EV-Mito) transfer mitochondria to brain microvascular endothelial cells: (a) Micrograph showing isolated EV-Mito from primary astrocyte (expressing mtD2) culture conditioned media. 10 µl used to image from 400 µl of concentrated EV-Mito derived from 15 ml of conditioned media. (b) Micrograph showing EV-Mito containing mitochondria (green) isolated from primary astrocytes expressing mtD2. (c) Micrograph showing EV-Mito isolated from WT astrocytes and stained for DAPI and tetramethylrhodamine ethyl ester (TMRE). (d) Micrograph showing transfered mitochondria (green) in BMECs using EV-Mito isolated from mtD2 primary astrocytes along with endogenous mitochondria (MitoTracker red; pink) after 48 h of incubation. (e) Micrograph showing transferred mitochondria (green) in mouse BMEC with endogenous mitochondria (TOM-20; pink) and wheat germ agglutinin (WGA; red) in mtD2 expressing-astrocyte and BMEC co-culture and (f) mtD2 expressing-astrocyte and BMEC co-culture showing the transfer of mitochondria from astrocyte to endothelial cells.

at locations where isolectin and mtD2 were present along with TOM-20 (endogenous mitochondria) in the absence of GFAP or AQP4 expression. Crucially, our capillary isolation method resulted in minimal astrocyte contamination, and even the few astrocyte remnants observed were mostly negative for mtD2. This represents a more robust and reliable way to quantify mitochondrial transfer to brain capillaries.

BMECs and pericytes form the BBB, protecting brain parenchymal cells from plasma proteins and other toxic substances through the action of efflux transporters located at the luminal and abluminal layers of the BBB.[24,26] The operation of these transporters requires substantial mitochondrial ATP. BMEC are constantly exposed to metabolites and waste products, making them susceptible to mitochondrial damage and reactive oxygen species (ROS) production.[36] Mitochondrial dysfunction in BMECs compromises tight junction proteins function and the integrity of BBB,[37,38] underscoring the critical role of healthy mitochondria. Astrocytes are shown to donate mitochondria to damaged neurons to support their recovery.[19,39,40] It is plausible that astrocytic mitochondrial transfer to BMECs is an indicator of the physiological energy demands necessary to maintain

mitochondrial homeostasis (mitostasis) or as a response to pathological mitochondrial dysfunction.

In the brain, intercellular transfer of mitochondria from astrocytes to neurons has been shown to rescue neurons from damage.[19,39] It has been recently reported that astrocytes also transfer mitochondria to brain endothelial cells, contributing to BBB integrity and angiogenic function.[30] As aging progresses, ROS and mitochondrial damage accumulate in BMEC.[35,41] To examine age-related changes in IMT between astrocytes and brain capillaries, we conducted a comparison of isolated brain capillaries from young and healthy-aged mice. Mitochondria have mitophagy-related turnover of around three weeks,[42,43] so transferred mtD2-labeled astrocytic mitochondria will not accumulate over time. Our results are therefore representative of transferred mitochondria from approximately the previous three weeks and we can attribute our findings to age-related alterations in IMT. We show there is increased astrocyte mitochondrial transfer in aging, which may suggest that IMT can serve to compensate for BMEC mitochondrial dysfunction in brain aging. However, this idea needs deeper investigation, as there is limited direct evidence to confirm the functional impact or participation of transferred mitochondria

in cellular recovery processes. Further research is essential to clarify whether the transferred mitochondria are indeed functional and capable of integrating into host cells to restore mitochondrial function.

Liu, et al. shows that aging reduces astrocytic mitochondrial transfer through decreased expression of Mitofusin 2 (MFN2), which is contrast to our findings.[30] There appear to be several caveats to this study, which may explain the difference in these major outcomes. The mouse model that was used (Dmp1-Cre) is not specific to astrocytes, as approximately 13.58% of smooth muscle cells are also Dmp1+ and other cells of the BBB can also express Dmp1.[30,44] Therefore, it is unclear whether the observed mitochondrial transfer originated from astrocytes or other cell types. Additionally, in the Lui, et al. study, Dmp1-Cre was intended to express Dendra2 specifically in astrocyte end-feet (AQP4+), and their confocal images indeed showed Dendra2 expression in astrocyte end-feet surrounding the capillaries. However, the quantification of mitochondrial transfer in brain sections was measured as Dendra2 co-localized with the endothelial cell marker (CD31), which makes it challenging to show transfer as up to 99% of the cerebrovascular surface is tightly covered by astrocytic end-feet.[45] Indeed, it is rare to find a location in brain sections where CD31 is positive and AQP4 is negative, highlighting the difficulty in distinguishing astrocyte end-feet from endothelial cells in these regions.

In addition to assessment of IMT in brain aging, we also wanted to examine EV-Mito mediated mitochondrial transfer between astrocytes and brain capillaries. One study found that interpericyte TNTs can shuttle mitochondria but do not transfer mitochondria between pericytes.[46] Our *in vitro* studies show that astrocyte and BMEC co-culture facilitates mitochondrial transfer from astrocytes to BMECs, consistent with previous findings.[29] Notably, our live cell imaging demonstrates that EV-Mito isolated from astrocytes can be used to efficiently transfer mitochondria to BMECs. Interestingly, *in vitro*, the transferred mitochondria appear to not fuse with the endogenous mitochondria and instead remain as a distinct pool for at least 72 hours. Another recent report shows that transplanted mitochondria do not fuse with the recipient pool.[47] While this phenomenon appears to occur in mitochondrial transplantation, it is unclear whether transferred mitochondria fuse with the recipient mitochondrial pool *in vivo*. Whether mitochondrial fusion occurs after IMT requires further experimentation, which could be facilitated with genetically-expressing astrocyte and endothelial/pericyte mitochondria with different fluorophores. These findings have implications for the delivery of respiratory-competent mitochondria in neurodegenerative diseases.[47,48]

Mitochondrial transplant is particularly promising, with applications in treating mitochondrial diseases, regenerating damaged tissues, and potentially reversing some degenerative conditions. However, the regulation, efficiency, and long-term effects of mitochondrial transplant remain areas of active research. Understanding the breadth and biological consequences of IMT could unlock novel strategies for pharmacological intervention and shed light on fundamental aspects of cellular communication and cooperation. Determining the functional state of transferred mitochondrial is a critical future direction for this area of research, which will offer insight into the purpose and mechanism of IMT. As research advances in mitochondrial transfer and uptake, mitochondrial transplantation stands poised to become a pivotal concept in cellular biology and therapeutic innovation.

In conclusion, we demonstrate mitochondrial transfer from astrocytes to BMEC and pericytes using the Ast-mtD2 animal model. We also find that this transfer occurs at low levels under physiological conditions and increases with aging. Importantly, our findings suggest that astrocyte-brain capillary mitochondrial transfer could potentially be mediated through EV-Mitos. Future studies are needed to determine if astrocytic to brain capillary IMT could serve as a compensatory mechanism to age-related vascular dysfunction. These results provide valuable insights and a potential strategy for designing astrocyte-based mitochondrial therapies to support brain capillary health in diseased or injured conditions.

Declaration of conflicting interests

The author(s) declared no potential conflicts of interest with respect to the research, authorship, and/or publication of this article.

Authors' contributions

GVV made initial observations. GVV and WBH developed the concept and designed the research. GVV performed the experiments, analyzed the data, interpreted the results of the experiments, prepared the figures and drafted the manuscript. WBH and PGS supervised all experiments. GVV, HJV, SPP, PGS, and WBH contributed substantially in editing and made critical revisions to the manuscript. WBH approved the final version of the manuscript.

Supplementary material

Supplemental material for this article is available online.

ORCID iDs

Gopal V Velmurugan ORCID https://orcid.org/0000-0003-2255-5931
W Brad Hubbard ORCID https://orcid.org/0000-0001-7018-0148

References

1. Dong LF, Rohlena J, Zobalova R, et al. Mitochondria on the move: Horizontal mitochondrial transfer in disease and health. *J Cell Biol* 2023; 222: e202211044.
2. Clemente-Suárez VJ, Martín-Rodríguez A, Yáñez-Sepúlveda R, et al. Mitochondrial transfer as a novel therapeutic approach in disease diagnosis and treatment. *Int J Mol Sci* May 2023; 24: 1.
3. Torralba D, Baixauli F and Sánchez-Madrid F. Mitochondria know No boundaries: mechanisms and functions of intercellular mitochondrial transfer. *Front Cell Dev Biol* 2016; 4: 107.
4. Liu D, Gao Y, Liu J, et al. Intercellular mitochondrial transfer as a means of tissue revitalization. *Signal Transduct Target Ther* 2021; 6: 65–1.
5. Brestoff JR, Wilen CB, Moley JR, et al. Intercellular mitochondria transfer to macrophages regulates white adipose tissue homeostasis and is impaired in obesity. *Cell Metab* 2021; 33: 270–282.e8.
6. Moschoi R, Imbert V, Nebout M, et al. Protective mitochondrial transfer from bone marrow stromal cells to acute myeloid leukemic cells during chemotherapy. *Blood* 2016; 128: 253–264.
7. Spees JL, Olson SD, Whitney MJ, et al. Mitochondrial transfer between cells can rescue aerobic respiration. *Proc Natl Acad Sci U S A* 2006; 103: 1283–1288.
8. Li H, Wang C, He T, et al. Mitochondrial transfer from bone marrow mesenchymal stem cells to motor neurons in spinal cord injury rats via gap junction. *Theranostics* 2019; 9: 2017–2035.
9. Babenko VA, Silachev DN, Popkov VA, et al. Miro1 enhances mitochondria transfer from multipotent mesenchymal stem cells (MMSC) to neural cells and improves the efficacy of cell recovery. *Molecules* 2018; 23: 687.
10. D'Souza A, Burch A, Dave KM, et al. Microvesicles transfer mitochondria and increase mitochondrial function in brain endothelial cells. *J Controlled Release* 2021; 338: 505–526.
11. Nicolás-Ávila JA, Lechuga-Vieco AV, Esteban-Martínez L, et al. A network of macrophages supports mitochondrial homeostasis in the heart. *Cell* 2020; 183: 94–109.e23.
12. Rustom A, Saffrich R, Markovic I, et al. Nanotubular highways for intercellular organelle transport. *Science* 2004; 303: 1007–1010.
13. Hough KP, Trevor JL, Strenkowski JG, et al. Exosomal transfer of mitochondria from airway myeloid-derived regulatory cells to T cells. *Redox Biol* 2018; 18: 54–64.
14. Kalluri R and LeBleu VS. The biology, function, and biomedical applications of exosomes. *Science* 2020; 367: eaau6977.
15. Borcherding N, Jia W, Giwa R, et al. Dietary lipids inhibit mitochondria transfer to macrophages to divert adipocyte-derived mitochondria into blood. *Cell Metab* 2022; 34: 1499–1513.e8.
16. Zhang S, Zhao D, Yang Z, et al. Circulating mitochondria promoted endothelial cGAS-derived neuroinflammation in subfornical organ to aggravate sympathetic overdrive in heart failure mice. *J Neuroinflammation* 2024; 21: 27.
17. Islam MN, Das SR, Emin MT, et al. Mitochondrial transfer from bone marrow-derived stromal cells to pulmonary alveoli protects against acute lung injury. *Nat Med* 2012; 18: 759–765.
18. Ahmad T, Mukherjee S, Pattnaik B, et al. Miro1 regulates intercellular mitochondrial transport & enhances mesenchymal stem cell rescue efficacy. *EMBO J* 2014; 33: 994–1010.
19. Hayakawa K, Esposito E, Wang X, et al. Transfer of mitochondria from astrocytes to neurons after stroke. *Nature* 2016; 535: 551–555.
20. Dong LF, Kovarova J, Bajzikova M, et al. Horizontal transfer of whole mitochondria restores tumorigenic potential in mitochondrial DNA-deficient cancer cells. *Elife* 2017; 6: e22187.
21. Watson DC, Bayik D, Storevik S, et al. GAP43-dependent mitochondria transfer from astrocytes enhances glioblastoma tumorigenicity. *Nat Cancer* 2023; 4: 648–664.
22. Lampinen R, Belaya I, Saveleva L, et al. Neuron-astrocyte transmitophagy is altered in Alzheimer's disease. *Neurobiol Dis* August 2022; 170: 105753.
23. Chen J, Zhong J, Wang LL, et al. Mitochondrial transfer in cardiovascular disease: from mechanisms to therapeutic implications. *Front Cardiovasc Med* 2021; 8: 771298.
24. Daneman R and Prat A. The blood–brain barrier. *Cold Spring Harb Perspect Biol* January 2015; 7: a020412.
25. Keaney J and Campbell M. The dynamic blood–brain barrier. *FEBS J* 2015; 282: 4067–4079.
26. Kadry H, Noorani B and Cucullo L. A blood–brain barrier overview on structure, function, impairment, and

biomarkers of integrity. *Fluids Barriers CNS* 2020; 17: 69–24.

27. Christie IN, Theparambil SM, Braga A, et al. Astrocytes produce nitric oxide via nitrite reduction in mitochondria to regulate cerebral blood flow during brain hypoxia. *Cell Rep* December 2023; 42: 113514.

28. Aten S, Kiyoshi CM, Arzola EP, et al. Ultrastructural view of astrocyte arborization, astrocyte-astrocyte and astrocyte-synapse contacts, intracellular vesicle-like structures, and mitochondrial network. *Prog Neurobiol* June 2022; 213: 102264.

29. Hayakawa K, Chan SJ, Mandeville ET, et al. Protective effects of endothelial progenitor cell-derived extracellular mitochondria in brain endothelium. *Stem Cells* 2018; 36: 1404–1410.

30. Liu D, Liao P, Li H, et al. Regulation of blood-brain barrier integrity by Dmp1-expressing astrocytes through mitochondrial transfer. *Sci Adv* 2024; 10: eadk2913.

31. Velmurugan GV, Vekaria HJ, Hartz AMS, et al. Oxidative stress alters mitochondrial homeostasis in isolated brain capillaries. *Fluids Barriers CNS* 2024; 21: 81.

32. Velmurugan GV, Hubbard WB, Prajapati P, et al. LRP1 deficiency promotes mitostasis in response to oxidative stress: implications for mitochondrial targeting after traumatic brain injury. *Cells* May 2023; 12: 1.

33. Schildge S, Bohrer C, Beck K, et al. Isolation and culture of mouse cortical astrocytes. *J Vis Exp* 2013; 50079.

34. Romeo R, Glotzbach K, Scheller A, et al. Deletion of LRP1 from astrocytes modifies neuronal network activity in an in vitro model of the tripartite synapse. *Front Cell Neurosci* 2020; 14: 567253.

35. Graves SI and Baker DJ. Implicating endothelial cell senescence to dysfunction in the ageing and diseased brain. *Basic Clin Pharmacol Toxicol* 2020; 127: 102–110.

36. Davidson SM and Duchen MR. Endothelial mitochondria: Contributing to vascular function and disease. *Circ Res* 2007; 100: 1128–1141.

37. Lee MJ, Jang Y, Han J, et al. Endothelial-specific Crif1 deletion induces BBB maturation and disruption via the alteration of actin dynamics by impaired mitochondrial

respiration. *J Cereb Blood Flow Metab* 2020; 40: 1546–1561.

38. Hubbard WB, Velmurugan GV, Brown EP, et al. Resilience of females to acute blood-brain barrier damage and anxiety behavior following mild blast traumatic brain injury. *Acta Neuropathol Commun* 2022; 10: 93.

39. English K, Shepherd A, Uzor NE, et al. Astrocytes rescue neuronal health after cisplatin treatment through mitochondrial transfer. *Acta Neuropathol Commun* 2020; 8: 36.

40. Li X, Li Y, Zhang Z, et al. Mild hypothermia facilitates mitochondrial transfer from astrocytes to injured neurons during oxygen-glucose deprivation/reoxygenation. *Neurosci Lett* 2021; 756: 135940.

41. Donato AJ, Machin DR and Lesniewski LA. Mechanisms of dysfunction in the aging vasculature and role in age-related disease. *Circ Res* 2018; 123: 825–848.

42. Menzies RA and Gold PH. The turnover of mitochondria in a variety of tissues of young adult and aged rats. *J Biol Chem* 1971; 246: 2425–2429.

43. Hu J, Cai M, Shang Q, et al. Elevated lactate by High-Intensity interval training regulates the hippocampal BDNF expression and the mitochondrial quality control system. *Front Physiol* February 2021; 12: 629914.

44. Jing B, Zhang C, Liu X, et al. Glycosylation of dentin matrix protein 1 is a novel key element for astrocyte maturation and BBB integrity. *Protein Cell* 2018; 9: 298–309.

45. Mills WA, Woo ALM, Jiang S, et al. Astrocyte plasticity in mice ensures continued endfoot coverage of cerebral blood vessels following injury and declines with age. *Nat Commun* 2022; 13: 1794–15.

46. Alarcon-Martinez L, Villafranca-Baughman D, Quintero H, et al. Interpericyte tunnelling nanotubes regulate neurovascular coupling. *Nature* 2020; 585: 91–95.

47. Lin RZ, Im GB, Luo AC, et al. Mitochondrial transfer mediates endothelial cell engraftment through mitophagy. *Nature* 2024; 629: 660–668.

48. Patel SP, Michael FM, Gollihue JL, et al. Delivery of mitoceuticals or respiratory competent mitochondria to sites of neurotrauma. *Mitochondrion* 2023; 68: 10–14.